THE ASTROPHYSICAL JOURNAL, 469:623–628, 1996 October 1

THE EARLY-TYPE DWARF-TO-GIANT RATIO AND SUBSTRUCTURE IN THE COMA CLUSTER

JEFF SECKER[1] AND WILLIAM E. HARRIS[2]
Department of Physics and Astronomy, McMaster University, Hamilton, Ontario, Canada L8S 4M1
Received 1995 December 4; accepted 1996 April 16

ABSTRACT

We have obtained new CCD photometry for a sample of $\simeq 800$ early-type galaxies (dwarf and giant ellipticals) in the central 700 arcmin^2 of the Coma cluster, complete in color and in magnitude to $R = 22.5$ mag ($M_R \simeq -12$ mag for $H_0 = 86$ km s^{-1} Mpc^{-1}). The composite luminosity function for all galaxies in the cluster core (excluding NGC 4874 and NGC 4889) is modeled as the sum of a Gaussian distribution for the giant galaxies and a Schechter function for the dwarf elliptical galaxies. We determine that the early-type dwarf-to-giant ratio (EDGR) for Coma is identical to that measured for the less rich Virgo cluster; i.e., the EDGR does not increase as predicted by the EDGR-richness correlation. We postulate that the presence of substructure is an important factor in determining the cluster's EDGR; that is, the EDGR for Coma is consistent with the Coma cluster being built up from the merger of multiple less-rich galaxy clusters.

Subject headings: galaxies: clusters: individual (Coma) — galaxies: evolution — galaxies: formation — galaxies: luminosity function

1. INTRODUCTION

In their seminal study of dwarf galaxy populations in nearby groups, Ferguson & Sandage (1991, hereafter FS91; Ferguson & Binggeli 1994) defined the early-type dwarf-to-giant ratio (EDGR) as the total number of early-type dwarf galaxies, N_d, normalized to the number of early-type giant galaxies, N_g. For the seven groups that they studied, they determined that the EDGR is strongly correlated with the richness of the group, in the sense that it increases monotonically with cluster richness and it appears to be independent of distance from the cluster center. This correlation should provide insights into both the initial formation of dE galaxies and environmental influences on their subsequent evolution. An excellent test of the EDGR correlation is to extend the analysis to much richer cluster environments than were originally surveyed in the studies mentioned above. Eventually, correlations with other cluster properties (e.g., X-ray luminosity, velocity dispersion, Bautz-Morgan class, substructure) can then be determined.

In their analysis, FS91 calculate the EDGR for four different luminosity limits in the range $M_{B_T} = -15.5$ to -12.5. In each case, N_d and N_g represent a sum of all early-type galaxies above that limiting magnitude: with N_g constant for all cases, the EDGR increases for fainter limiting magnitudes. FS91 assigned galaxies in several nearby groups and clusters into morphological classes using visual inspection from photographic plates. By definition, they assign $N_d = N$(dE + dE, N + dS0) and $N_g = N$(E + S0). In their analysis, the most convincing demonstration of the EDGR-richness correlation was obtained by using N_g itself as a measure of the cluster richness. Then a plot of N_d versus N_g shows clearly that the number of dwarfs rises faster than the number of giants: the ratios N_d/N_g for Fornax and Virgo (Abell richness class 1, two of the richest clusters in their study) are clearly larger than for Leo, Dorado, and NGC 1400 (the poorest groups).

In a separate study of dwarf galaxies near early-type galaxies, Vader & Sandage (1991) confirmed the observed correlation for the EDGR to increase with environment richness. They found that giant galaxies in the richest groups are typically ~ 2 times overabundant in companion dE galaxies when compared to the mean value of their sample. In contrast, isolated field galaxies are typically ~ 10 times underabundant in dE companions relative to the sample mean. It is worthwhile to note here that the definition of richness used by FS91 and Vader & Sandage (1991) differs from the Abell richness class. Abell (1958) defined his "richness class" as a number in the range 0–5, corresponding to the number of counted galaxies that are not more than 2 mag fainter than the third brightest member. This scheme allows considerable variation in numbers and densities within individual richness classes, and, for consistency, it requires imaging of the entire cluster field. The FS91 definition of richness as equivalent to log N_g provides an alternative method for ordering groups by richness, provided again that a considerable and consistent fraction of the cluster is measured.

The Coma cluster is the nearest of the very rich Abell clusters (Abell 1956, richness class 2, $v \simeq 7000$ km s^{-1}). In this paper, we describe new luminosity and color data for the galaxies in the cluster core, which allow us to define the EDGR accurately. In § 2, we summarize the observations and the derivation of the EDGR. In § 3, we discuss some implications of our data, particularly an interpretation of EDGR-richness correlation in the context of cluster merger and observed substructure.

2. THE EARLY-TYPE DWARF-TO-GIANT RATIO

Our new CCD photometry is described fully in Secker (1995, hereafter S95) and Secker & Harris (1996, hereafter SH96). In brief, the KPNO 4 m telescope was used in 1991 April to mosaic image the central region of the Coma cluster in two colors (B, R), with the prime-focus camera and the TE 2K CCD detector. The total area covered was $\simeq 700$ arcmin^2, which included a field centered on each of NGC 4874 and NGC 4889, and one extending nearly 23′ south of NGC 4874. A control field located about 2°.1 east

[1] Present address: Washington State University, Program in Astronomy, Pullman, WA 99164-3113.
[2] Visiting Astronomer, KPNO, which is operated by AURA, Inc., under contract with the National Science Foundation.

of NGC 4874 was also imaged, in order to facilitate statistical correction of the background population. Total exposure times were 2700 s for both R and B, with the seeing between 1".1 and 1".3. Since our targets were E and dE galaxies (characteristically old stellar populations), we detected objects on the R-band images, which had a slightly deeper limiting magnitude for these moderately red objects. Total magnitudes for all detected objects on the frames were determined by a curve-of-growth algorithm (i.e., apertures of radius $2r_1$; see S95), and they were tested for systematic correctness by extensive Monte Carlo simulations of the images. Analysis also showed that detections of faint galaxies are $\gtrsim 80\%$ complete to $R = 22.5$ mag: brighter than this limit, (minor) completeness corrections are made to the measured luminosity function of the detected objects; anything fainter than this limit was discarded so as to keep only the highest confidence data. Furthermore, we are complete in $B-R$ to this same level. Typical uncertainties near our completeness limits are ± 0.06 mag in R and ± 0.12 mag in $B-R$.

Concerning our detection completeness of dwarf galaxies, we will comment on the two cases involving spatially extended giant galaxies, near which our detection of dwarf galaxies is generally quite a bit more incomplete. In the end, we conclude that this spatial incompleteness does not strongly affect our computed EDGR.

1. *Very near to brightest giants.*—While a bias against detecting close companion galaxies in a cluster environment such as Coma certainly exists in wide-field data such as this, we note that the majority of the dwarf galaxy population is not gravitationally bound to any of the giant galaxies (Binggeli 1993; Ferguson 1992; Vader & Chaboyer 1992). Thus, we do not expect this bias to affect our computed EDGR since the affected area is quite small in total.

2. *Within an arcmin of the supergiant galaxies NGC 4874 and NGC 4889.*—As detected by SH96 and by Bernstein et al. (1995), the radial number density profiles for dE galaxies increase toward NGC 4874. However, Thompson & Gregory (1993, hereafter TG93) determined that for their sample of bright dE galaxies, this radial profile could be scaled downward (in central surface density) in such a way as to match that of the early-type giant galaxies. This is a direct indication that the EDGR is constant with position in the cluster (provided that the limiting magnitude to which the dE galaxies are counted is not too faint; see SH96). This result of TG93 is analogous to the result of FS91 for the Virgo cluster, viz., that the EDGR is independent of clustercentric radius. Thus, the true EDGR for the two excluded regions around the supergiant galaxies is consistent with our computed value for the cluster core, within fluctuations owing to small number statistics arising from the small area concerned. (Note that these two incomplete regions comprise a mere $\simeq 1.6\%$ of the total area studied.)

The process of eliminating contaminating objects (foreground stars and noncluster galaxies) was done in two parts. Nonstellar objects were reasonably well resolved in a parameter space of r_{-2} (an image moment that sensitively measures central concentration; see S95; SH96) versus total magnitude R. The sequence of starlike objects in this plane ($r_{-2} \lesssim 1.6$ pixels) brighter than $R = 19.5$ mag is easily distinguished, and these bright starlike objects were discarded. (This is only a minor correction, since the overwhelming majority of detected objects in the Coma field are nonstellar, faint galaxies.) Next, the R, $(B-R)$ color-magnitude diagram of all the remaining objects was used to remove the noncluster galaxies from the sample. In this diagram (see Fig. 1), it is clear that the Coma galaxies populate a narrowly defined sequence, confined (conservatively) to the range $0.7 \leq B-R \leq 1.9$ mag. We discarded any objects outside of this color range, leaving a total of 2526 candidate galaxies ($R \leq 22.5$ mag) in the cluster core, compared to 694 objects on the control field. With a total area 2.57 times less than the cluster field area, the control-field number density is 2.56 ± 0.10 objects arcmin^{-2}.

A comparison of our background number density with other similar studies is worthwhile. Prior to color discrimination but within the same magnitude range, our sample of control-field objects numbered 1146, or a number density of 4.23 objects arcmin^{-2}. By comparison, Bernstein et al. (1995) derive an R-band control-field number density given by 5.46 objects arcmin^{-2}, over the same magnitude range. (This number corresponds to an average over five randomly located control fields, and not related to the position of the Coma cluster.) In his analysis of field galaxies, Koo (1986) derived a mean galaxy number density of 3.69 arcmin^{-2} to a magnitude cutoff of 22.5 mag in the F filter (their red bandpass) in a field located near to (but outside of) the Coma cluster. Thus, prior to imposing the color constraints, our computed background number density is comparable to other derived values. This comparison clearly illustrates the benefits of deriving colors for all detected objects: the level of contamination by background objects is greatly reduced, without affecting the population of true cluster galaxies.

The expected luminosity range for all types of dwarf galaxies is fainter than $R \simeq 15.5$ mag, and, as illustrated in Figure 1, these objects are generously included in our survey. We do not attempt to divide these dwarf galaxies into their morphological subgroups (nucleated and nonnucleated dEs, irregulars, etc.), simply because we have

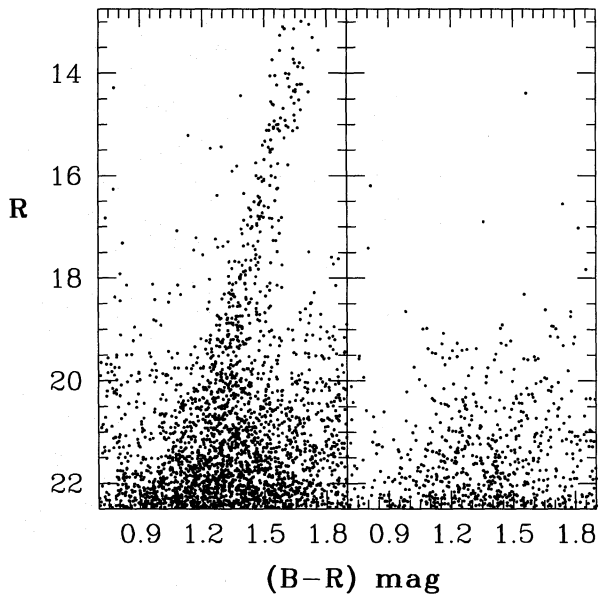

FIG. 1.—Color-magnitude diagrams (CMDs) for detected objects on the cluster fields (*left panel*) and on the control field, which is 2° from the cluster center (*right panel*). The cluster galaxies (dwarf and giants) are immediately obvious as a sequence of objects that are restricted to a narrow range in $B-R$ color, and which are not present on the control field CMD.

insufficient spatial resolution. However, the vast majority of our sample must be dwarf ellipticals uncontaminated by late-type systems. In their analysis of late-type dwarf (dIr) galaxies in Coma, TG93 find a significant decrease in the number density of dIr galaxies in the Coma cluster core, with typical values of 14–40 dIr deg^{-2} to $R \lesssim 18.6$. Scaling these densities to our 0.194 deg^2 field, we therefore expect only 3–8 dIrs to this limit, considerably less than the number of dE galaxies (see Table 2). Fainter than this, the luminosity function for dIr galaxies is bounded (Binggeli, Sandage, & Tammann 1988), unlike the still-rising luminosity function for dE galaxies.

Brighter than $R \simeq 15.5$, our sample includes all detected giant galaxies, excluding only the supergiants NGC 4874 and NGC 4889. While the number of late-type giants in the cluster core is small, it is not negligible. Thompson & Gregory (1980) detect a total of 34 spiral galaxies in a 1.49 deg^2 region of the cluster core; hence, in our sample we would expect 2–7 spirals. However, since we cannot individually separate and discard the late-type dwarf galaxies, we do not discard the few late-type giants either. Thus, we are assuming that the contaminating late-type galaxies compose similar fractions of the bright and faint galaxy populations. While this late-type dwarf-to-giant ratio is *slightly less* than the EDGR for rich clusters (FS91), the effect of sample contamination by late-type galaxies on the computed EDGR will be small when averaged in with the much larger sample of early-type galaxies.

In both previous analyses, FS91 and TG93 used visual classification to separate galaxies into their morphological subgroups, with surface brightness as the primary discriminator between giants and dwarfs. TG93 and, more recently, Biviano et al. (1995) determined that the composite luminosity function (LF) for the Coma cluster is well fitted by a Gaussian distribution for the bright cluster members and a Schechter function for the dwarf galaxies. The sum of these two functions, with the appropriate normalization, has been found to provide a better representation of the total luminosity function than a single Schechter function. Conveniently, the resulting scaled functions provide the *relative contribution to the LF by each of the dwarf and giant galaxy populations.* It is this technique that we adopt in principle to determine the EDGR value for our sample of cluster galaxies.

The net galaxy LF, which we analyze here, is plotted in Figure 2, where the number of galaxies per 0.5 mag bin is represented by the solid circle and the associated error bars. Both the raw galaxy LF and the background field LF were first corrected for small incompleteness effects using a completeness function derived from the overlapping regions of the three adjacent Coma fields (i.e., the sample is essentially 100% complete to the 18th magnitude, falling gradually to 80% complete at 22.5 mag). The error bars for the net LF plotted in Figure 2 represent the Poisson errors from the two individual LFs added in quadrature.

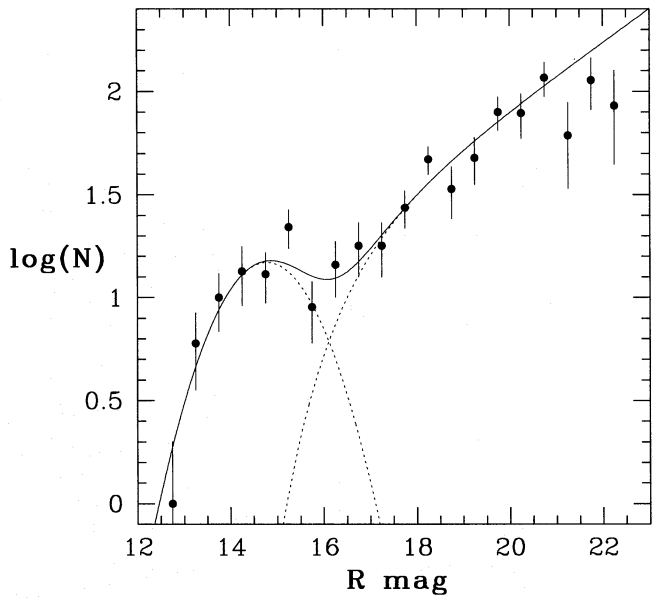

FIG. 2.—The composite galaxy luminosity function (LF) for the Coma cluster core. Solid dots represent the total number of Coma galaxies (after correction for incompleteness and background subtraction) per half-magnitude bin. The solid line shows the model fit, the sum of two separate contributions (*dashed lines*) from the giants (i.e., a log-normal distribution) and dwarf ellipticals (i.e., a Schechter function). In this plot, we illustrate model fit 3, for which the Gaussian distribution has a dispersion of $\sigma = 1.0$ mag; the other relevant parameters are given in Tables 1 and 2. The three faintest points were not included in the fit, as they adversely affect normalization over the region of interest.

Weighted least-squares fits of a Gaussian plus a Schechter function to the luminosity function of Figure 2 then allowed us to solve for the relative contribution from each of the giant and dwarf galaxy populations. This fit formally involves six parameters: the peak magnitude m^0, dispersion σ, and normalization κ_1 of the Gaussian function for the giants; and the characteristic magnitude m^*, the faint-end slope α, and normalization κ_2 of the Schechter LF for the dwarf galaxies. However, two of these parameters (σ, α) can be reasonably constrained a priori. A separate analysis of the faint-end slope of our LF yields $\alpha = -1.41 \pm 0.05$ (SH96; and consistent with TG93 and Bernstein et al. 1995),

TABLE 1

FITS OF THE GAUSSIAN-PLUS-SCHECHTER MODEL TO THE GALAXY LUMINOSITY FUNCTION

	GAUSSIAN			SCHECHTER			
FIT	κ_1	m^0	σ	κ_2	m^*	α	χ^2/ν
1	15.30 ± 9	14.53 ± 0.01	0.80	14.74 ± 19	15.61 ± 0.37	−1.41	0.87
1a	14.29 ± 13	14.48 ± 0.01	0.80	9.89 ± 21	15.10 ± 0.91	−1.46	0.85
1b	16.01 ± 7	14.57 ± 0.01	0.80	19.95 ± 20	15.97 ± 0.21	−1.36	0.93
2	15.18 ± 7	14.66 ± 0.01	0.90	17.30 ± 24	15.96 ± 0.31	−1.41	0.86
3	14.82 ± 6	14.78 ± 0.01	1.00	19.58 ± 29	16.23 ± 0.28	−1.41	0.90
4	14.40 ± 6	14.90 ± 0.01	1.10	21.57 ± 35	16.44 ± 0.26	−1.41	0.98
5	14.04 ± 5	15.04 ± 0.01	1.20	23.33 ± 41	16.61 ± 0.26	−1.41	1.06
5a	13.72 ± 6	15.01 ± 0.01	1.20	18.08 ± 40	16.37 ± 0.41	−1.46	1.09
5b	14.30 ± 5	15.05 ± 0.01	1.20	28.98 ± 44	16.82 ± 0.18	−1.36	1.04

TABLE 2

N(dE + DE, N + DS0) AND THE EDGR FOR DIFFERENT FUNCTION FITS AND LIMITING MAGNITUDES

R-MAG LIMIT	N(dE + dE, N + dS0) 1	1a	1b	2	3	4	5	5a	5b	COMA EDGR	VIRGO EDGR
18.6.....	66.9	67.8	66.5	62.3	58.2	54.7	51.7	51.3	51.6	1.80 ± 0.58	2.12
19.6.....	120.1	120.7	120.0	116.2	112.4	109.0	106.0	104.7	106.4	3.38 ± 0.86	3.61
20.6.....	199.7	202.8	197.0	197.5	195.0	192.5	190.2	190.4	188.6	5.80 ± 1.33	5.77
21.6.....	316.8	328.9	305.9	317.6	317.5	316.9	316.0	323.8	306.6	9.41 ± 2.14	9.31

NOTE.—N(E + S0) is calculated over the range $12.5 \leq R \leq 18.5$ mag, and equals 30.51, 28.46, 31.95, 33.96, 36.72, 39.11, 41.42, 40.44 and 42.20 for fits 1 through 5b (as above). The Virgo EDGR values are taken from FS91.

and we limit the Gaussian dispersion to lie within the realistic range $\sigma = 1.0 \pm 0.2$ mag (see TG93; Biviano et al. 1995). The numerical results corresponding to nine separate cases are summarized in Table 1; on the basis of the reduced χ^2 values, any of these can be accepted on statistical grounds. The model fits corresponding to extreme values for σ and α will define upper and lower limits to the EDGR, while the adopted EDGR represents the average of these extreme values. For all models considered here, the maximum EDGR is for the smallest σ combined with a steep faint-end slope (i.e., fit 1a), while the minimum EDGR is for the largest σ combined with a shallow faint-end slope (i.e., fit 5b).

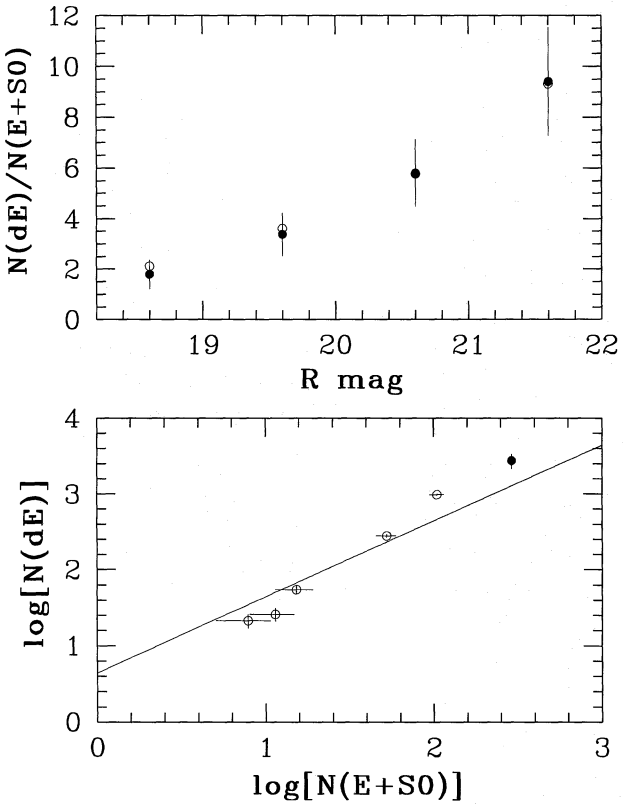

FIG. 3.—Early-type dwarf-to-giant ratio (EDGR) for the Coma cluster. In both panels, the solid circle corresponds to our measured EDGR for the Coma cluster. In the top panel, it is clear that the Coma and Virgo EDGRs are identical within the uncertainties (those shown are for our computed values) for the four different magnitude limits used in the numerical integration of the Schechter function. In the lower panel, we plot the number of early-type dwarf galaxies (to a $R = 21.6$ mag limit) vs the number of early-type giant galaxies. From left to right, the open circles represent Leo, Dorado, NGC 1400, Fornax, and Virgo (from FS91), while the solid dot is the Coma value from our study, and the solid line has a slope of unity.

As mentioned above, the calculation of the EDGR involves numerically integrating the Schechter function to an arbitrary limiting magnitude. To remain consistent with the limiting magnitudes used by FS91, it is necessary to convert our apparent R total magnitudes to their absolute total magnitudes M_{B_T}. To do so, we adopt the same parameters used by TG93: a difference in distance moduli [d(Coma-Virgo)] of 3.68 mag and B-band K-corrections of 0.12 mag for Coma and 0.02 mag for Virgo. To this we add the Virgo distance modulus of 31.7 used by FS91.[3] Finally, we adopt a mean dE color of $B-R = 1.4$ mag for $R \simeq 18.0$ (S95; SH96). This leads to a conversion factor, from our R mag to a M_{B_T} mag on the FS91 scale of $M_{B_T} \simeq R - 34.1$. Then the four limiting magnitudes that we adopt are $R = 18.6$, 19.6, 20.6, and 21.6 mag, corresponding to their $M_{B_T} = -15.5$, -14.5, -13.5, and -12.5 mag limits.

We integrate the Gaussian function over the interval $12.5 \leq R \leq 18.5$ mag, and we obtain values for the number of giants of N(E+S0) = 30.51, 28.46, 31.95, 33.96, 36.72, 39.11, 41.42, 40.44, and 42.20 for model fits 1, 1a, 1b, 2, 3, 4, 5, 5a, and 5b, respectively. In Table 2, we provide the corresponding number of dwarfs N(dE+dE N+dS0) and the Coma EDGR values, obtained by numerically integrating the Schechter function over the appropriate magnitude ranges using the parameter values relevant to the five different fits. In Figure 2, we illustrate one of the model fits (i.e., fit 3, with $\sigma = 1.0$ mag and $\alpha = -1.41$) to the composite luminosity function. The dotted lines designate the individual contributions from the dwarfs and giants, while the solid line is the direct sum of the two.

Throughout this paper, we have discussed the uncertainties inherent in our method and assumptions. Here we briefly review these: (*a*) the dispersion of the Gaussian distribution is varied through the range $\sigma = 1.0 \pm 0.2$ mag, consistent with observations; (*b*) the faint-end slope of the Schechter function is varied through the range $\alpha = -1.41 \pm 0.05$, consistent with this and other analyses; (*c*) Poisson variations in the LF of faint background objects are accounted for; (*d*) possible overestimates of the EDGR, which could result from the inclusion of late-type dIr galaxies in the sample, are counterbalanced by a similar fraction of late-type giants, which are also present in the sample (both late-type dwarfs and giants are present only at a very low level); and (*e*) the completeness function is involved in the correction of both the program field and the control field LF, although at such a low level that plausible variations in it would have only a small effect. Of these factors,

[3] This is not the Virgo distance modulus that we would adopt. Its only purpose here is to transform their absolute magnitudes back to appropriate *apparent* magnitudes at the Coma distance.

(*a*) and (*b*) dominate the uncertainty estimates on our estimate of the Coma EDGR.

Of immediate interest is whether our computed EDGR for the Coma cluster exceeds that measured for Virgo, and, therefore, if the EDGR-richness correlation continues to this still-richer environment. In the top panel of Figure 3, we compare our derived EDGR values for the Coma cluster (i.e., *solid circles*, from Table 2) with those computed for Virgo (i.e., *open circles*; FS91). These two sets of values are entirely consistent at all four limiting R magnitudes. This reflects the fact that the faint-end slopes of the galaxy LF are similar in both clusters. Note that to a limit of $R = 18.6$ mag, TG93 measured an EDGR of 1.50, slightly lower than (but formally consistent with) our value. While the primary difference between our values results from the modeling of the log-normal distribution (TG93 fix $\sigma = 1.2$ mag), it must also be caused by the inclusion of lower surface brightness dE galaxies in our deeper CCD sample (S95; SH96).

In the bottom panel of Figure 3, we plot the EDGR (calculated to a limit of $R = 21.6$ mag) for five galaxy groups taken from FS91. To place Coma on this figure at the correct richness, we adopt $N(\mathrm{E}+\mathrm{S0}) = 291$ (TG93) as a measure of the total number of giants in the entire Coma cluster. Adopting this value places Coma as easily the richest galaxy cluster in this sample, in agreement with the Abell richness class rankings. Then we use a Coma EDGR equal to 9.41 ± 2.14 (Table 2), in such a way as to scale the number of measured dwarf galaxies for the cluster core to the Coma cluster as a whole. In this manner, we can put our derived EDGR for the Coma cluster on the richness scale used by FS91 and Vader & Sandage (1991; i.e., $\log N_g$).

In the bottom panely of Figure 3, the solid line has unit slope, representing a constant EDGR with increasing cluster richness: the Fornax, Virgo, and Coma clusters clearly lie well above this line, while the Leo, Dorado, and NGC 1400 groups fall below. Then from Figure 3 and Table 2, *the EDGR value for the Coma cluster is consistent with that found for the Virgo cluster, within our calculated uncertainties*, and it is clearly lower than would have been expected if the EDGR was to keep increasing monotonically with cluster richness.

3. DISCUSSION

Rich galaxy clusters exhibit considerable variation within individual richness classes, including properties such as: (1) the velocity dispersion of the member galaxies; (2) the Bautz-Morgan class, which measures the magnitude difference between the first- and second-ranked cluster galaxies; (3) the presence or absence of a central cD galaxy, (4) X-ray emission; and (5) evidence for significant substructure. Substructuring, in particular, must clearly be an important factor in determining the early-type dwarf-to-giant ratio. For example, if two or more richness-class 1 galaxy clusters merge to form a richer cluster, then to first order the total number of dwarf and giant galaxies will be conserved, and the EDGR for the new (richer) cluster will mimic those for the original subclusters, rather than being larger, as suggested by the basic correlation shown in Figure 3. Thus, the simple EDGR-richness correlation must really represent an EDGR-richness-subcluster correlation (if not other parameters too). We are not suggesting that substructure replaces the dependence on richness: there remains an EDGR-richness correlation for *original* groups and clusters. However, substructure can explain why the EDGR for *merger-product* clusters can mimic the EDGR of the less-rich subgroups, instead of being as rich as predicted by the EDGR-richness correlation.

For the case of Coma and Virgo, our results are consistent with a scenario in which identifiable subgroups in these clusters are richer than the sparse clusters in the FS91 sample of poor groups, and they are consistent with the Coma cluster being the result of a significant number of merger events (e.g., Fitchett & Webster 1987; Escalera, Slezak, & Mazure 1992; Davis & Mushotzky 1993; Mohr, Fabricant, & Geller 1993; White, Briel, & Henry 1993; West, Jones, & Forman 1995; Colless & Dunn 1996). We postulate that to find an EDGR value that is clearly larger than the Coma and Virgo values, it will be necessary to survey a cluster environment that is rich *by birth*, rather than by subsequent growth. To turn this statement around, we suggest that a clear signature of the very richest, densest galaxy environments (and by extension, the most massive cluster potential wells in the early universe) should be the presence of a significantly higher EDGR than Coma or Virgo. Thus, for the EDGR-richness correlation to be relevant to the formation and evolution of dE galaxies and the galaxy cluster itself, we must disentangle the effects of richness and substructure.

Finally, SH96 discusses two additional factors affecting the EDGR for rich galaxy clusters: (1) variation of the EDGR with clustercentric radius, due to the destruction of faint dEs in the dense core, and (2) a predicted increase in the EDGR with cluster X-ray luminosity, resulting from a confinement pressure exerted by dense intracluster gas on proto-dE galaxies—i.e., more of the young dwarf elliptical galaxies in gas-poor clusters should have expelled their metal-rich gas and subsequently faded (see Babul & Rees 1992). Further surveys of other, more distant rich galaxy clusters to trace out these effects would be of great interest.

This research was supported in part by the Natural Sciences and Engineering Research Council of Canada, through a grant to W. E. H., and by the Ontario Ministry of Colleges and Universities, through an Ontario Graduate Scholarship to J. S. We would like to thank an anonymous referee for helpful comments, and we would like to acknowledge the assistance of Stephen Holland with the observations.

REFERENCES

Abell, G. O. 1958, ApJS, 3, 211
Babul, A., & Rees, M. J. 1992, MNRAS, 255, 346
Bernstein, G. M., Nichol, R. C., Tyson, J. A., Ulmer, M. P., & Wittman, D. 1995, AJ, 110, 1507
Binggeli, B. 1993, Habilitationsschrift, Univ. Basel
Binggeli, B., Sandage, A., & Tammann, G. A. 1988, ARA&A, 26, 509
Biviano, A., Durret, F., Gerbal, D., Le Fèvre, O., Lobo, C., Mazure, A., & Slezak, E. 1995, A&A, 297, 610
Colless, M., & Dunn, A. M. 1996, ApJ, 458, 435
Davis, D. S., & Mushotzky, R. F. 1993, AJ, 105, 409
Escalera, E., Slezak, E., & Mazure, A. 1992, A&A, 264, 379
Ferguson, H. C. 1992, MNRAS, 255, 389
Ferguson, H. C., & Binggeli, B. 1994, A&A Rev., 6, 67-122
Ferguson, H. C., & Sandage, A. 1991, AJ, 101, 765 (FS91)
Fitchett, M., & Webster, R. 1987, ApJ, 317, 653
Koo, D. C. 1986, ApJ, 311, 651
Mohr, J. J., Fabricant, D. G., & Geller, M. J. 1993, ApJ, 413, 492
Secker, J. 1995, Ph.D. thesis, McMaster Univ. (S95)
Secker, J., & Harris, W. E. 1996, in preparation (SH96)
Thompson, L. A., & Gregory, S. A. 1980, ApJ, 242, 1

Thompson, L. A., & Gregory, S. A. 1993, AJ, 106, 2197 (TG93)
Vader, J. P., & Chaboyer, B. 1992, PASP, 104, 57
Vader, J. P., & Sandage, A. 1991, ApJ, 379, L1
West, M. J., Jones, C., & Forman, W. 1995, ApJ, 451, L5
White, S. D. M., Briel, U. G., & Henry, J. P. 1993, MNRAS, 261, L8

Note added in proof.—According to L. A. Thompson (1996, personal communication), the EDGR computed by Thompson & Gregory (1993) was incorrect by a factor of 78.0/67.0 (see their eqs. 1b and 1c). The published value should be 1.75 and not 1.50. The value of 1.80 computed in this paper is consistent with their corrected value.